

EXPERIMENTAL INVESTIGATION OF BOND BETWEEN FRP AND CONCRETE

Baolin Wan, University of South Carolina, Columbia, SC
Dr. Michael F. Petrou, University of South Carolina, Columbia, SC
Dr. Kent A. Harries, University of South Carolina, Columbia, SC
Dr. Michael A. Sutton, University of South Carolina, Columbia, SC
Dr. Bangcheng Yang, University of South Carolina, Columbia, SC

Abstract

Modified double cantilever beam (MDCB) specimens are used to evaluate bond toughness between E-glass FRP overlay and common concrete substrate in this study. A customized test frame was built for this test. The equations used to calculate the energy release rate G are developed. A computer vision system for measuring crack location, near-tip deformations and crack opening displacement is introduced and demonstrated. The digital image correlation method is used to find the crack opening displacement (COD) for flaws growing in the vicinity of the FRP-concrete bond. Results from the study indicate that the value of G and local Mode I COD increase with the increased of the proportion of concrete on the crack surface, with the measured local Mode II COD being relatively low and constant throughout the crack growth process.

Introduction

The use of fiber reinforced polymer (FRP) composite materials for infrastructure rehabilitation and retrofit applications has been widely studied. The advantages of FRP composite materials include high specific stiffness and specific strength ratios, outstanding fatigue behavior, corrosion resistance, and ease of handling.

The failure modes of reinforced concrete having externally applied FRP retrofit measures can be grouped into six distinct categories (Buyukozturk et al., 1998): steel yield and FRP rupture, concrete compression failure, shear failure, failure of cover concrete along reinforcing steel layer (splitting), delamination of FRP material and peeling of FRP material due to shear distortions and cracking. The delamination and peeling modes are directly related to the properties of the bond between the FRP and concrete substrate.

Since structural performance relies on the bond between FRP and concrete, the characteristics of the bond and methods to evaluate it are critical to understanding and evaluating FRP retrofitting techniques, their behavior and failure mechanisms. Methods previously used to investigate FRP bond to concrete include: uniaxial tension tests (Steele, 1994; Mullins et al., 1998), peel tests (Karbhari and Engineer, 1996, 1997), direct and torsion shear tests (Mullins et al., 1998), four-point bending tests (Kurtz, 2000), and modified double cantilever beam tests (Giurgiutiu et al., 2001; Lyons et al., 2001).

Another parameter that has potential in quantifying the performance of the bond between FRP and concrete is crack opening displacement (COD). This is particularly true since the bond between FRP and concrete may be mixed mode, and a true mixed mode COD can be measured using non-contacting methods such as computer vision. In this regard, recent mixed mode fracture studies for aerospace alloys have shown that a critical COD at a specific distance behind the crack tip is a viable parameter for predicting crack growth in various levels of Mode I and II (Amstutz et al, 1995; Dawicke et al, 1995; Sutton et al 2000-2, Sutton et al 2000-3) and Mode I, II and III (Sutton et al, 2001, Helm et al, 2001).

Research Significance and Objectives

The objective of this study is to demonstrate the applicability of using a computer vision system and modified double cantilever beam specimens to evaluate the bond between FRP and a concrete substrate. Two parameters, interfacial energy release rate, G , and crack opening displacement (COD) are used to evaluate the properties of the FRP bond to the concrete substrate.

Background and Theory

Energy Release Rate of Modified Double Cantilever Beam Test

The Modified Double Cantilever Beam (MDCB) test was developed by Giurgiutiu et al. (2001). The specimens used in the MDCB are made by bonding a composite overlay to a concrete or masonry substrate. Debonding the overlay from the substrate beginning at one end and progressing along the specimen results in the “double cantilever”: one cantilever is the debonded overlay, the other is the substrate material. The composite overlay is significantly more compliant than concrete substrate. In the development of the equations for the energy release rate of the interface between FRP and concrete, the concrete substrate is assumed to be rigid and all of the strain energy is stored in the FRP overlay.

The specimen used in this study is illustrated in Figure 1. The interfacial energy release rate, G , of MDCB is expressed as (Lyons et al, 2001; Naik et al., 1989):

$$G = \frac{3m^3P^2(a_{\text{exp}} + \frac{n}{m} - \Delta_s)^2}{2B} \quad (1)$$

where P is the external load applied to the FRP overlay as a Mode I loading, a_{exp} is the crack length measured from the experiment, B is the width of the specimen, Δ_s is the shortening of the crack length due to the effects of large deflections, and m and n are determined from experimental data from Equation 2.

$$C^{1/3} = ma_{\text{exp}} + n \quad (2)$$

where m is the slope of the line given by equation 2, and n is the intercept with the $C^{1/3}$ axis. C is the compliance of the FRP overlay which is expressed as:

$$C = \frac{\delta}{P} \quad (3)$$

where δ is the vertical displacement of the load point.

Computer Vision

Computer vision is a non-contacting, surface deformation measurement method used for the study of solid structures. In-plane deformation on planar surfaces and 3D deformations on other planar or curved surfaces can be measured by using 2D and 3D digital image correlation methods, respectively. The theories and various applications of DIC-2D and DIC-3D are well documented in two recent book chapters (Sutton et al., 1999 and 2000-1).

Experimental Investigation

Materials

The FRP material used in this initial study is a commercially available unidirectional woven E-Glass fabric having an areal weight of 900 g/m^2 (27 oz/yd^2). The manufacturer's reported longitudinal modulus, E_{11} , of the raw fiber is 72.4 GPa (10.5 Msi) and the thickness of one ply is reported as 0.4 mm (0.016 in.). An epoxy-base saturant, provided by the E-Glass manufacturer comprises the matrix and provides the bond to the concrete substrate. Previous material characterization of the same FRP material system (Harries and Kharel, 2001) report the longitudinal modulus of the layed-up FRP to be 4.9 kN/mm-ply (28 kips/in-ply). Due to lay-up variation, it is difficult to obtain a consistent thickness and, as a result, modulus values, in traditional units. Thickness units of "ply" or layers of FRP fabric are adopted for simplicity.

The concrete substrate was a normal weight, portland cement concrete. The substrate was primed with a thin layer of saturant prior to the application of the FRP material.

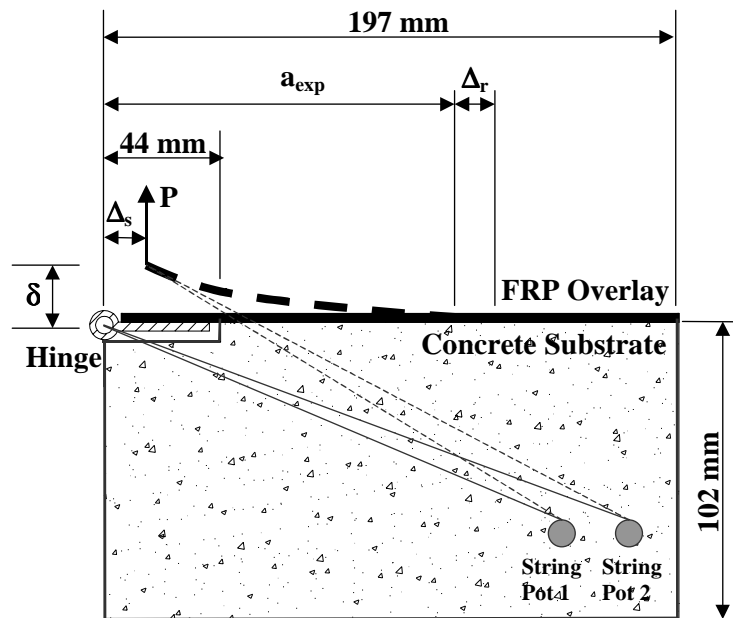


Figure 1. Schematic of the test method and the specimen (width = 76 mm).

Specimens

A concrete block was built and two plies FRP were applied to the block. At the same time, hinges were bonded to the FRP. After the FRP cured, the block was cut using a concrete saw into four separate specimens. Using this method, variance of properties and lay-up between specimens is reduced.

The substrate concrete for each specimen is $76 \times 102 \times 197 \text{ mm}$ ($3 \times 4 \times 7.75 \text{ in.}$) as shown in Figure 1. On the surface to which the FRP is to be applied, a 44-mm (1.7 in.) long by 6-mm (0.25 in.) deep gap was provided. This gap serves as the initial crack and permits the hinge to lie flat (see Figure 1).

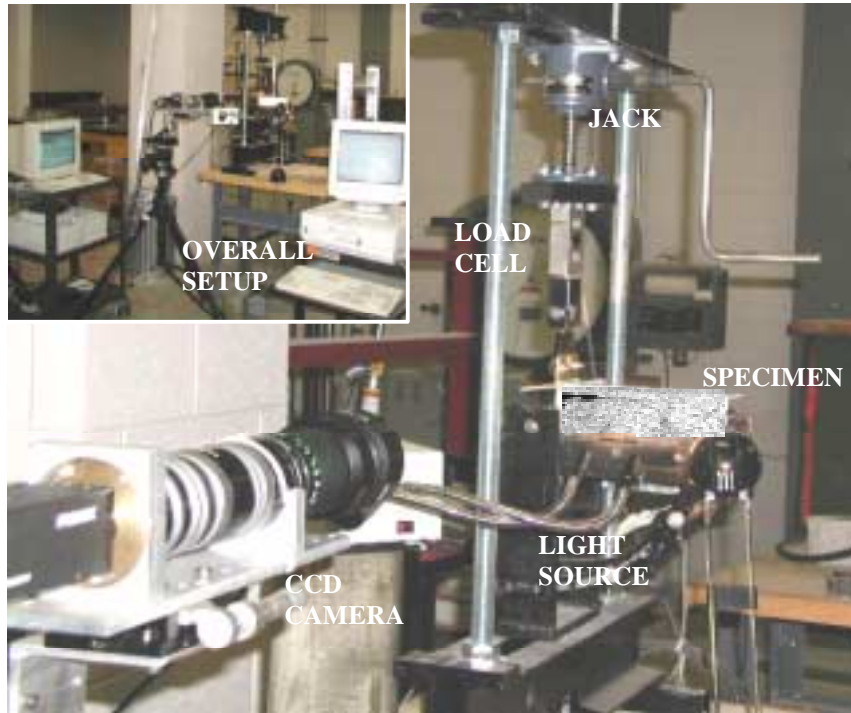


Figure 2. Test setup.

Test Setup and Instrumentation

A customized test frame was built for this test. The load, P , is applied using a 8.8 kN (2000 lb) screw jack. A 13.3 kN (3000 lb) universal load cell is used to record the load. The test setup is shown in Figure 2.

Two string potentiometers are used to the one side of the specimen to trace the position of the loading point. As shown in Figure 1, the distance between the potentiometers is fixed and the distances between the loading point and the string pots are measured. The horizontal and vertical displacements of the loading point are then calculated by trigonometry. A data acquisition system was used to collect the data of load and loading positions.

Experimental Setup for Computer Vision and COD Measurement

A photograph of the camera system and test setup used in this work to measure COD is shown in Figure 2. As shown in this figure, a digital camera is mounted on a three-dimensional translation stage so that the camera can be translated with the crack tip region and images of the crack-tip region acquired during the stable tearing process.

To use existing computer software for image analysis (VIC-2D), a random black and white pattern having a spot size of approximately $45\ \mu\text{m}$ is applied to the specimen surface using commercial enamel spray paints. During the test, a 7mm X10mm region around the current crack tip location is imaged using a combination lens system with the CCD camera; a 200mm Canon FD lens and two-2X-extenders are used to obtain a typical image magnification of 70-90 pixels/mm for all specimens. Loading is performed in displacement control until surface crack growth is observed on the video monitor. At this point, images of the crack tip region are obtained either as the current crack front begins to advance or just after incremental crack growth occurs. Figure 3 shows two of the images used in this work to quantify COD during crack growth. After an image has been acquired, the load-point displacement is increased and the process repeated until unstable crack growth occurred.

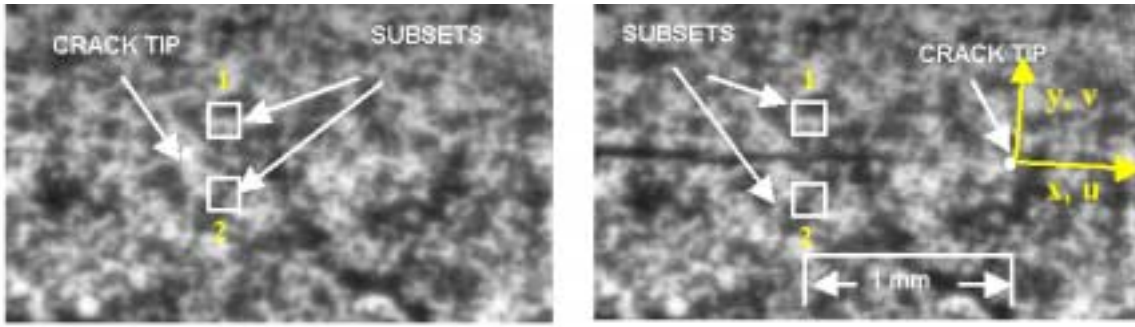


Figure 3. Location of subsets in crack-tip region for crack opening displacement (COD) measurement.

Crack Opening Displacement Measurement

After acquiring images of the crack at various stages of growth, two subsets are selected at approximately 1 mm behind the current crack tip and along the crack line (see Figure 3). By comparing the subset locations in two images using custom image analysis software (VIC-2D), the relative displacements between the two subsets can be quantified and COD measured. As in previous work, COD is the relative crack surface displacement at 1mm behind the current crack tip and can be written in the form:

$$\text{COD} = \sqrt{(u_2 - u_1)^2 + (v_2 - v_1)^2} \quad (4)$$

where u_i and v_i are components of crack surface displacement perpendicular and parallel to the local crack line at a distance of 1mm behind the current crack tip. Thus $(u_2 - u_1)$ is the local mode I component of COD (COD_{I}), $(v_2 - v_1)$ is the local mode II component of COD (COD_{II}) and Equation 4 gives the total relative crack surface displacement (COD).

In this manner, post-processing of images taken during the stable crack growth process is used to measure COD_{I} , COD_{II} so that the total COD can be computed as a function of crack extension.

Observations from Investigation

Energy Release Rate

The energy release rate of a typical specimen is calculated using Equation 1 and is shown in Figure 4. The photo of the crack surfaces after complete removal of the FRP is also shown in the figure. It can be seen in the figure that the value of interfacial energy release rate, G , is low when the crack propagates in the interface between the FRP and concrete. When the crack path passes partially through the interface and partially through the concrete, the value of G becomes higher. For the crack length between 120 to 160 mm, the value of G increases along with the increased of the proportion of concrete on the crack surface. This clearly indicates that the substrate concrete has a higher energy release rate than the bond along the interface. At values of crack length, a_{exp} , greater than 160 mm, the crack passes totally in the concrete. The values of G at these locations are not as high as expected. The crack in these locations is very unstable and the assumed boundary condition of a fixed end at the crack tip is not valid near the end of the specimen. It is not expected that the relationship expressed in Equation 1 is valid as the crack length approaches the end of the specimen.

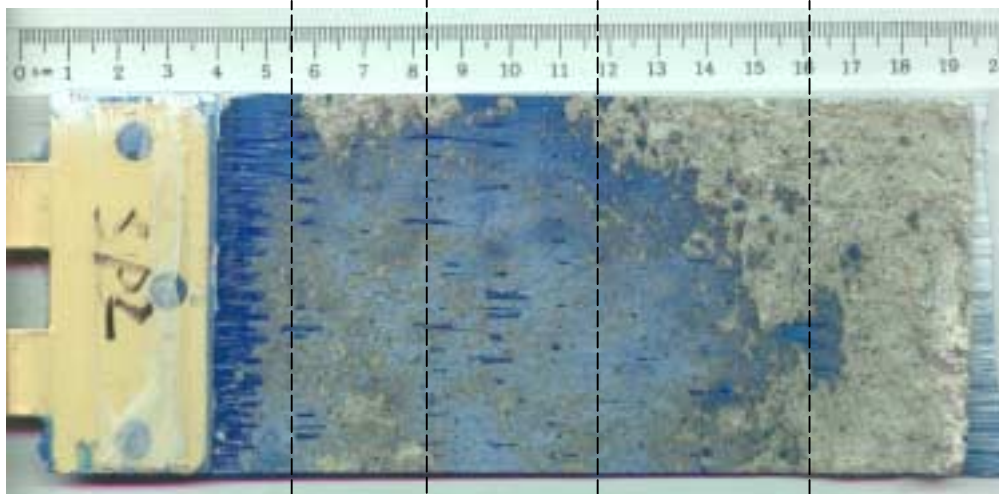
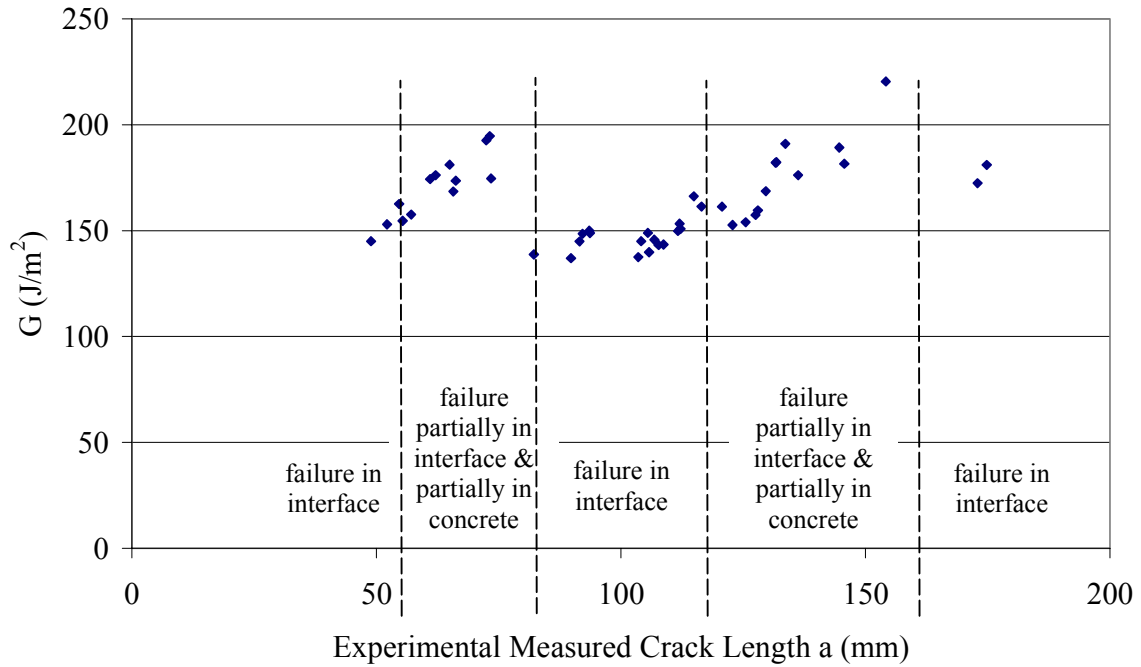


Figure 4. Interfacial energy release rate vs. experimental measured crack length for a typical specimen.

Effect of Large Deflection

The maximum value of G calculated using Equation 1 including geometric nonlinearity in the form of the term Δ_s for the example specimen is 181 J/m^2 . A simple linear calculation, neglecting Δ_s results in a G value of 188 J/m^2 . This indicates that the nonlinear effect due to large deflections is not particularly significant in these tests. This result agrees with the conclusion of the research of Naik et al. (1989) that the effect of large deflections in a hinged DCB is small.

Crack Opening Displacement Measurement

As noted previously, digital images for the tests were analyzed by using digital image correlation software to obtain both COD and the amount of crack growth. The amount of crack growth can be defined as either the extension along the actual crack path (Δa) or the projection of Δa onto a horizontal axis parallel to original crack line (Δx). Though both values are reported, the difference between these two values is small for the specimens tested in this work.

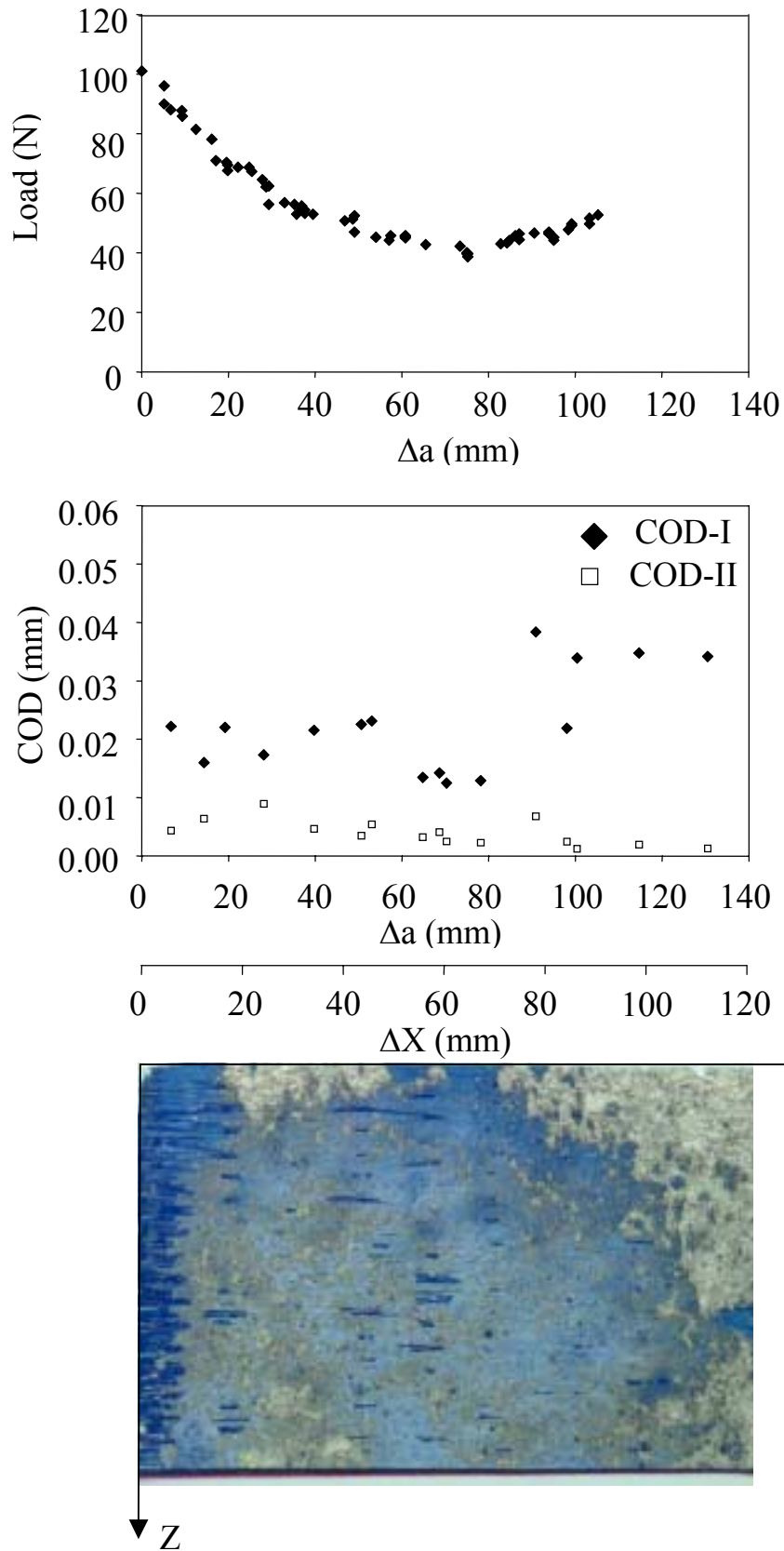


Figure 5. Load, COD-crack extension data and corresponding fracture surface for a typical specimen.

Typical COD-crack extension data and load-crack extension results are shown in Figure 5. The load-crack extension data show that maximum load corresponds to crack initiation, with nearly monotonic load reduction during stable crack extension. Note that the monotonic load reduction continues, even though fracture may occur along the interface, within the concrete or in a combination of interface and concrete along the crack front. Such behavior is consistent with brittle fracture processes.

It is also noted that the COD_I and COD_{II} data indicate the mode II component of COD is relatively small throughout the crack growth process. Thus, even though the FRP overlay is undergoing large deformations during the peel test, the results suggest that local mode I conditions are dominant in the crack tip region.

For all specimens in this study, the presence of concrete as a function of crack extension was determined by visual inspection of enlarged digital images of the fracture surface. The percentage of concrete as a function of crack length was determined by qualitatively estimating the area of concrete in a 1mm wide rectangular strip extending across the entire specimen width. Using this approach, Figure 6 relates the measured total COD to the percentage of concrete on the fracture surface. Note that this method for relating concrete percentage to COD implicitly assumes a straight crack front.

Figure 6 shows that COD is directly related to the percentage of concrete on the fracture surface; COD increases correspondingly with the increasing of concrete percentage. Specifically, the data indicates that (a) COD is nearly constant with a mean of 0.019mm and a standard deviation of 0.004 mm when the concrete percentage is within 0~10 %, b) COD is nearly constant with a mean of 0.033 mm and a standard deviation of 0.003 mm when the percentage of concrete is greater than 50% and (c) a transition region of substantial variability exists when the percentage of concrete is between 10% and 50% of the fracture surface. Thus, the critical COD is a minimum when the crack grows within the FRP-concrete interface (concrete percentage is less than 10%). Similarly, the critical COD is a maximum when at least 50% of the fracture surface is within the concrete.

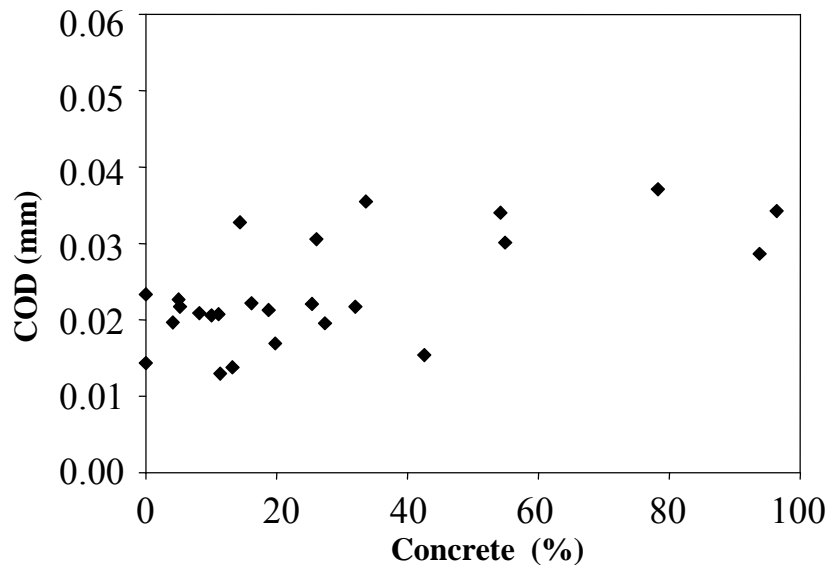


Figure 6. COD as function of percentage of concrete on the crack surface.

Conclusions

Modified double cantilever beam specimens were used to investigate the fracture behavior of the bond region between FRP and concrete. Crack growth and crack opening displacement were acquired through a computer vision system and image analysis software. Based on experimental observations, the following conclusions are attained:

1. A novel computer vision methodology is successfully used to measure mixed mode COD for a flaw growing near the FRP-concrete interface
2. The measured values for mixed mode COD indicate that the flaw is growing in predominantly mode I conditions, with a small component of mode II COD remaining constant throughout the growth process.
3. The measured values for mixed mode COD and G are related to the percentage of concrete on the fracture surface; increasing as the percentage of concrete on the fracture surface increases. The behavior suggests threshold values of COD may be expressed as a function of the percentage of concrete on the fracture surface.

Acknowledgements

This research is supported by the South Carolina Department of Transportation and the National Science Foundation (CMS 9908293).

References

1. Amstutz, B.E., Sutton, M.A. and D.S. Dawicke (1995) "Experimental Study of Mixed Mode I/II Stable Crack Growth in Thin 2024-T3 Aluminum", *Fatigue and Fracture*, Vol. 26; *ASTM STP 1256*, P256-273.
2. Buyukozturk, O. and Hearing, B. (1998), "Failure Behavior of Precracked Concrete Beams Retrofitted with FRP," *Journal of Composites for Construction*, August 1998, P138-144.
3. Dawicke, D.S., Newman III, J.C., Sutton, M.A. and Bigelow, C. (1995) "Orientation Effects on the Measurement and Analysis of Critical CTOA in an Aluminum Alloy", *Fatigue and Fracture*, *ASTM STP 1256*, P243-256.
4. Giurgiutiu, V., Lyons, J., Petrou, M.F., Laub, D. and Whitley, S. (2001), "Fracture Mechanics Testing of the Bond between Composite Overlays and Concrete Substrate," *Journal of Adhesion Science and Technology*, 2001, P.
5. Harries, K.A., and Kharel, G. (2002), "Behavior of Variably Confined Concrete" accepted for publication in *ACI Materials Journal*. (in press)
6. Helm, J.D., Sutton, M.A. and Boone, M.L., (2001) "Characterizing Crack Growth in Thin Aluminum Panels Under Tension-Torsion Loading with Three-Dimensional Digital Image Correlation", *Nontraditional Methods of Sensing Stress, Strain and Damage in Materials and Structures*, *ASTM STP 1323*, P3-14.

7. Karbhari, V.M. and Engineer, M. (1996), "Investigation of Bond Between Concrete and Composites: Use of a Peel Test," *Journal of Reinforced Plastics and Composites*, Vol. 15, February 1996, P208-227.
8. Karbhari, V.M., Engineer, M. and Eckel II, D.A. (1997), "On the Durability of Composite Rehabilitation Schemes for Concrete: Use of a Peel Test," *Journal of Material Science*, Vol. 32, 1997, P147-156.
9. Kurtz, S.J. (2000), *Failure Criteria for Reinforced Concrete Beams Strengthened with Carbon Composites*, Dissertation, State University of New Jersey, October 2000.
10. Lyons, J, Laub, D., Giurgiutiu, V., Petrou, M.F. and Salem, H. (2001), "Effect of Hygrothermal Aging on the Fracture of Composite Overlays on Concrete," *Journal of Reinforced Plastics and Composites*, Vol. 20, No. 00/2001.
11. Mullins, G., Sen, R. and Spain, J. (1998), "Testing of CFRP/Concrete Bond," *Second International Conference on Composites in Infrastructure*, Tucson, AZ 1998, P211-218.
12. Naik, R.A., Crews, J.H. and Shivakumar, K.N. (1989), "Effect of T-Tabs and Large Deflections in Double Cantilever Beam Specimen Tests," *ASTM Special Technical Publication*, November 1989, P169-186.
13. Steele, J. (1994), "Testing Adhesion of Coatings Applied to Concrete," *Materials Performance*, Vol. 33, No. 11, November 1994, P33-36.
14. Sutton, M.A., McNeill, S.R., Jang, J. and Babai, M. (1988) "The Effects of Sub-pixel Image Restoration on Digital Correlation Error Estimates", *Optical Engineering*, Vol. 27, No. 3, P173-175.
15. Sutton, M.A., McNeill, S.R., Helm, J.D. and Chao, Y.J., (1999) "Advances in Two-dimensional and Three-dimensional Computer Vision", Photomechanics, Springer Verlag, Topics in Applied Physics, Vol. 77, P323-372
16. Sutton, M.A., McNeill, S.R., Helm, J.D. and Chao, Y.J., (2000) "Trends in Optical Non-Destructive Testing and Inspection, Ed. By Rastogi, P and Inaudi, D., P571-591
17. Sutton, M.A., Ma, F. and Deng, F. (2000) "Development and Application of a CTOD-Based Mixed Mode Fracture Criterion", *International Journal for Solids and Structures*, Vo.37, P3591-3618.
18. Sutton, M.A, Boone, M.L., Ma, F. and Helm, J.D. (2000) "A combined modeling-experimental study of the crack opening displacement criterion for characterization of stable crack growth under mixed mode I/II loading in thin sheet materials", *Engineering Fracture Mechanics*, Vol. 66, P171-185.
19. Sutton, M.A., Helm, J.D. and Boone, M.L. (2001) "Experimental Study of Crack Growth in Thin Sheet Material under Tension-Torsion Loading", *International Journal of Fracture*, Vo.109, P285-301.
20. VIC-2D Image Analysis software, Correlated Solutions, Incorporated, West Columbia, SC 29169.